Turk J Phys
33 (2009) , 201 – 208.

doi:10.3906/fiz-0811-9

The electrical conduction mechanisms and thermoelectric power of SnSe single crystals

M. M. NASSARY
Physics Department, Faculty of Science, South Valley University, Qena-EGYPT
e-mail: Nassary_99@yahoo.com

Received 14.11.2008

Abstract

Single crystals of SnSe were prepared in our laboratory by a special modified Bridgman technique. Measurements of the electrical conductivity and Hall effect between 141 K and 553 K were carried out on SnSe sample in two crystallographic directions. The investigated sample was found to be of p-type conductivity. The Hall mobilities parallel and perpendicular to layers plane at room temperature, were 7835.9 cm^2 / V·s and 7274.7 cm^2 / V.s, respectively. The free carrier concentration $P = 3.52 \times 10^{12}$ cm^{-3} at room temperature. Also, the thermoelectric power (TEP) was investigated in the temperature range from 176 to 553 K. The relations between the thermoelectric power and the concentration of charge carriers and electrical conductivity were studied. Mobilities, effective masses, relaxation times, diffusion lengths and diffusion coefficients both for majority and minority carriers were obtained at room temperature.

Key Words: SnSe Single crystal, Hall Coefficient, thermoelectric power.

1. Introduction

SnSe belongs to the group of layer-type orthorhombic structure with eight atoms per unit cell forming double-layer planes normal to the longest axis with space group D_{2h}^{16}. Previously, the absorption edge [1–4], infrared and Raman spectra [5], and electroreflectance and thermoreflectance [6] have been studied. The band structure was first calculated by Car et al [7], Ciucci et al [8] and by Gashimzade et al [9]. SnSe has the lattice constants $a = 0.419$ nm, $b = 0.446$ nm and $c = 1.157$ nm [10]. The core excitations and conduction band structures [11], infrared and Raman spectra [12, 10], electron-energy-loss spectroscopy [13] and energy band structure [14] and dispersion analysis [15] have been investigated for SnSe. Due to the anisotropic character of SnSe, the optical and electrical measurements on these materials have been performed by polarized light.

2. Experimental measurements

Details of the experiment equipment for growth by the Bridgman-Stockbarger technique have been reported elsewhere [21]. The materials were supplied from Aldrich with a purity of 99.999% both for selenium and tin. 7.913 g of tin (60.05 %) and 5.264 g of selenium (39.947 %) were used as starting materials in this experiment. The single crystals were grown in evacuated quartz ampoule at 10^{-5} Torr. The ampoule with its charge was introduced into a three-zone tube furnace. At the beginning of the growth, the ampoule was held in the first zone of the furnace at 1183 K for about 24 h. Melt homogenization was done in this zone where the temperature is higher than the melting point. Via a very slow rate of movement, the ampoule, with its charge, was made to enter the second zone of the furnace where the temperature equaled that of the crystallization point [16]. Finally, solidification occurs in the third zone. Such processes need about eleven days for one to have single crystals of SnSe compound. The produced ingot was identified by means of X-ray analysis to be a SnSe crystal. The results were in good agreement with published values [17] recorded in the International Centre for Diffraction Data (ICDD) standard.

For studying the electrical conductivity and Hall effect, the sample was prepared in a rectangular shape with dimensions $5.75 \times 2 \times 1.25$ mm^3. Silver paste contact was used as ohmic contact. Since metal-semiconductor contacts generate voltage, the I-V characteristic were recorded in two different directions. The results showed that silver paste is a good ohmic contact. The conductivity and the Hall coefficient were measured by a compensation method in a special cryostat [18] with a conventional D.C. type measuring system by using a Tinsley UJ33E potentiometer in a 0.5 T magnetic field. The temperature range of investigation was extended from 141 K up to 553 K. All measurements were carried out under vacuum condition of about 10^{-3} Torr.

For studying the thermoelectric power (TEP), an evacuated calorimeter (10^{-3} Torr) was used to protect the sample from oxidation and water vapor condensation at high and low temperatures, respectively. The calorimeter has two heaters. The outer heater (the external source) discharges its heat slowly to the specimen environment. The inner heater (connected to the lower end of the crystal) was made purposely to control the temperature and its gradient along the specimen. The TEP is calculated at different temperatures by dividing the magnitude of the thermal voltage difference across the crystal by the temperature difference between the hot and cold ends.

3. Results and discussion

3.1. Temperature dependence of electrical conductivity and Hall effect

The temperature dependence of electrical conductivity of SnSe single crystal sample was studied in the two crystallographic directions over temperature range 141 K to 553 K. Figure 1 shows the variation of the electrical conductivity parallel and perpendicular to the layers ($\sigma_{||}$, $\perp\sigma_{\perp}$) with temperature. These curves are quite similar to the semiconductor behavior. From this figure, three regions are obtained. In the first region, found at low temperature, 141–358 K and 141–322 K, the electrical conductivities ($\sigma_{||}$,s$\sigma_{\perp}$) parallel and perpendicular to layers, respectively, increase slowly due to the extrinsic region in which the carrier concentration is determined by the number of ionized acceptors. The existence of an intermediate region, which extends from 358–478 K and 322–518 K for directions parallel and perpendicular to the layers ($\sigma_{||}$, $\sigma_{\perp}$),

respectively, corresponds to the impurity exhaustion range. In this range all the impurity atoms are ionized but no noticeable excitation of intrinsic carriers take place. The third region from 478–553 K and 518–553 K for directions parallel and perpendicular ($\sigma_{||}$, $\sigma_{\perp}$) to the layers, respectively, represents the intrinsic region. In this region the conductivities $\sigma_{||}$ and $\sigma_{\perp}$ increase rapidly by increasing temperature because of the carrier being excited from the extended state of the valence band into the conduction band. From the slope of this region the energy gap $E_{g||}$ and $E_{g\perp}$ can be calculated. It is found to be $E_{g||} = 0.98$ eV and $E_{g\perp} = 0.25$ eV. The value of $E_{g||} = 0.98$ eV is in good agreement with the value reported previously, $E_g = 0.9$ eV [5, 19]. The room temperature conductivity of the sample is $4.42 \times 10^{-3}\ (\Omega \cdot cm)^{-1}$ and $6.9 \times 10^{-3}\ (\Omega \cdot cm)^{-1}$ for directions parallel and perpendicular to the layers plane, respectively.

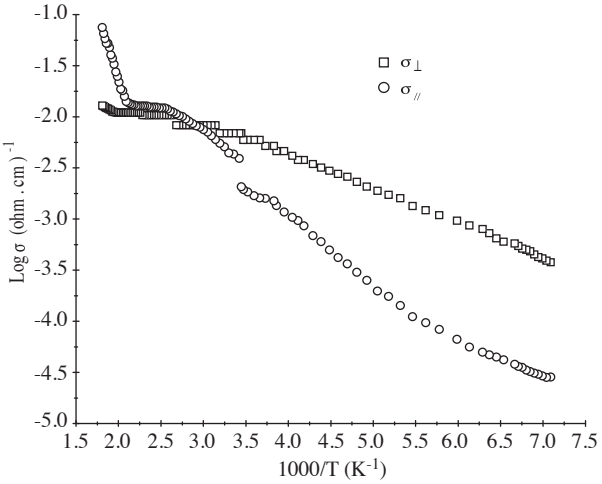

Figure 1. Temperature dependence of the electrical conductivity for SnSe single crystal.

Figure 2 shows the relation between $R_H T^{3/2}$ and $10^3/T$. From the results calculated from this figure we can conclude that:

1. The positive sign of R_H indicates p-type conductivity.
2. This curve can be evaluated into three regions.

The first region in the temperature range, 141–478 K, expresses the extrinsic region. The second region in the temperature range, 478–518 K, expresses the transition region. The third region at high temperature expresses the intrinsic region. From the slope of this part, the energy gap is calculated to be $E_g = 0.91$ eV. This value is also in a good agreement with the conductivity measurements. A combination of the Hall measurements and the electrical conductivity data were used to study the temperature dependence of the mobility of the charge carriers in the two directions parallel and perpendicular to the layers plane.

Figure 3 indicates the relation between the carrier mobilities $\mu_{||}$, $\mu_{\perp}$ and temperature T. The relation $\mu_H \alpha T^n$ governs the variation of the Hall mobility as a function of temperature. This curve distinguishes three regions for $\mu_{||}$ and two regions for $\mu_{\perp}$. In the first region, at law temperatures 141–208 K for $\mu_{H||}$, $\mu_{H\perp}$, the mobilities $\mu_{H||}$, $\mu_{H\perp}$ increases with temperature following curves related to $\mu_{||} \alpha T^2$ and $\mu_{\perp} \alpha T^{3.9}$, respectively. These results indicate that the scattering mechanism is essentially due to the ionized impurities. The second region in the temperature range from 208–468 K for $\mu_{H||}$, $\mu_{H\perp}$. In this temperature range the $\mu_{H||}$ decreases

with increasing temperature following a curve related to $\mu_{||}\alpha T^{-3.15}$. This is due to acoustic phonon scattering. In contrast $\mu_{H\perp}$ increases slightly with increasing temperature, following a curve related to $\mu_{H\perp}\alpha T^{1.1}$. In the third region in the temperature range from 468 K to 553 K the Hall mobility $\mu_{H||}$ increases with temperature by relation $\mu_{H||}\alpha T^{10.5}$. The value of n and its sign suggests that the scattering mechanism of carriers differ from that in semiconductor materials. Such anomalous behavior can be explained neither by classical theories of semiconductors nor by the concept of acoustic phonon scattering based on Schmid's model [20]; but for $\mu_{H\perp}$ seems to be fairly constant with temperature. The mobility carriers at room temperature parallel and perpendicular to the layers plane equal 7835.9 $\mathrm{cm}^2/\mathrm{V}\cdot\mathrm{s}$ and 7274.7 $\mathrm{cm}^2/\mathrm{V}\cdot\mathrm{s}$, respectively. Figure 4 represents the dependence of charge carrier concentration on temperature. The charge carrier concentration was calculated from Hall data using the relation $P = 1/R_H e$ where, P is hole concentration, e is electron charge. From this figure we notice that the concentration of carriers in the extrinsic region increases slowly with increasing temperature, while it increases rapidly with temperature in the intrinsic region. The energy gap calculated from the slope of this curve in the high temperature range is found to be $E_g = 0.98$ eV. The hole concentration at room temperature is $P = 3.52 \times 10^{12}\ \mathrm{cm}^{-3}$.

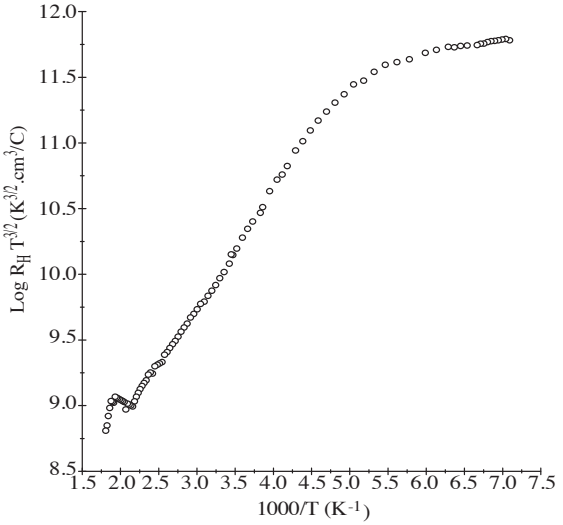

Figure 2. Relation between $R_H T^{3/2}$ and $10^3/T$ for single crystal.

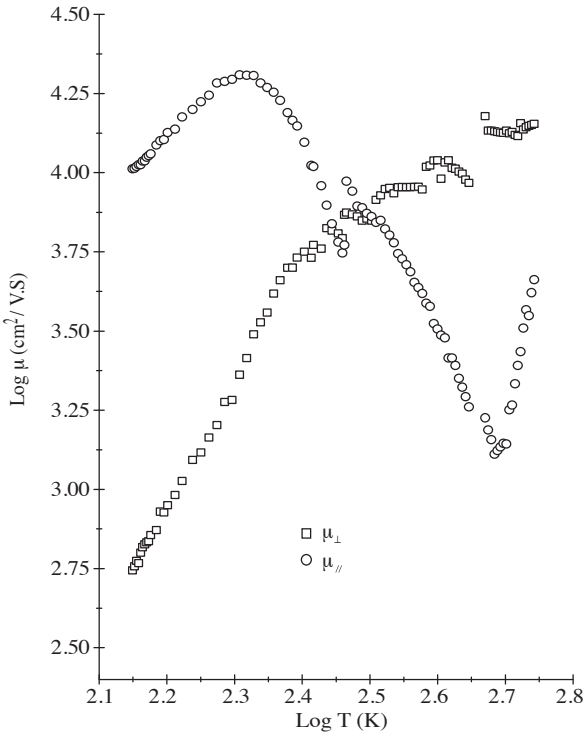

Figure 3. The behavior of Hall mobility as a function of temperature for SnSe single crystal.

3.2. Temperature Dependence of Thermoelectric Power of SnSe

The thermoelectric power (TEP) measurements were performed with the direction of temperature gradient parallel to the layers plane over a wide temperature range, 176–553 K. Figure 5 illustrates the general

behavior of the variation of the TEP with temperature. From this curve, the Seebeck coefficient α seems to be fairly constant with increasing the temperature up to the temperature 272.5 K. Above this temperature, the value of α increases as the temperature rises. The thermoelectric coefficient at room temperature equal to 19.3 $\mu V/K$. The high values of α in the intrinsic conductivity region may be a result of the effect of phonon drag on the charge carriers [21]. It is evident from these measurements that α has a positive sign in the whole temperature range of investigation. This is in agreement with results obtained from Hall data.

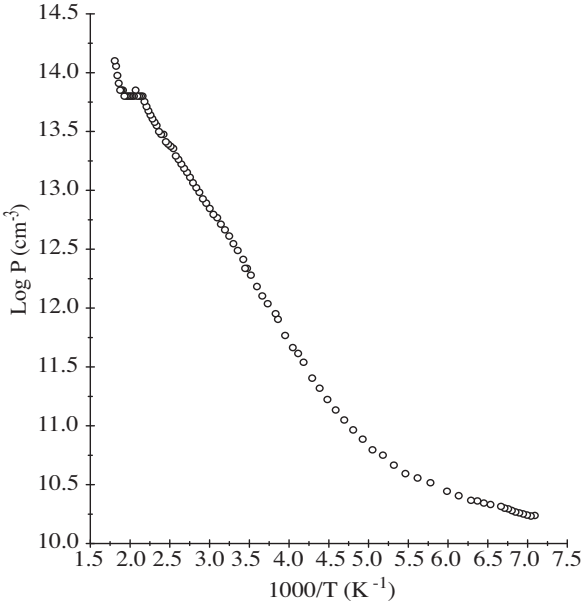

Figure 4. Variation of hole concentration with temperature for SnSe single crystal.

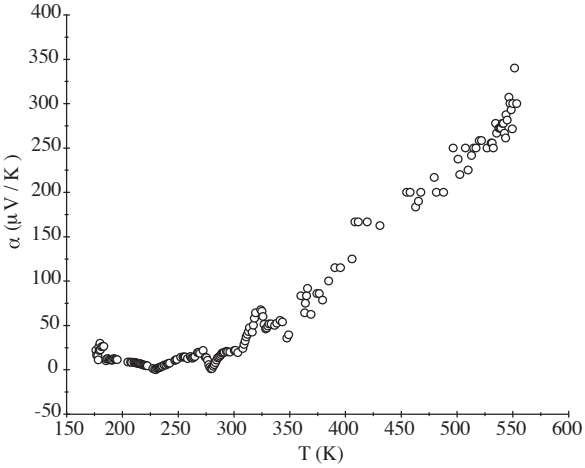

Figure 5. Temperature dependence of thermoelectric power for SnSe single crystal.

The behavior of thermoelectric power with temperature in the intrinsic region can be described by the equation given by Lauc [22]:

$$\alpha = -\frac{k}{e}\left[\frac{b-1}{b+1}\left(\frac{\Delta E_g}{2kT}+2\right)+\frac{1}{2}Ln\left(\frac{m_n^*}{m_p^*}\right)^{3/2}\right] \tag{1}$$

where, b is the ratio of electron to hole mobility, E_g is the energy gap, k is the Boltzmann constant and m_n^*, m_p^* are the effective mass of electron and hole, respectively. The relationship shows that a plot of α in the intrinsic range as a function of the reciprocal of absolute temperature is a straight line, as shown in Figure 6. The slope of the linear part is used to estimate the ratio of the electron to hole mobility. Taking $E_{g||} = 0.98$ eV, from the previously obtained data, the ratio $b = \mu_n/\mu_p$ is found to be 2.91. Hence by using the value of $\mu_p = 7835.7\ \mathrm{cm}^2/\mathrm{V}\cdot\mathrm{s}$, the electron mobility can be deduced and its value is found to be $22802\ \mathrm{cm}^2/\mathrm{V}\cdot\mathrm{s}$.

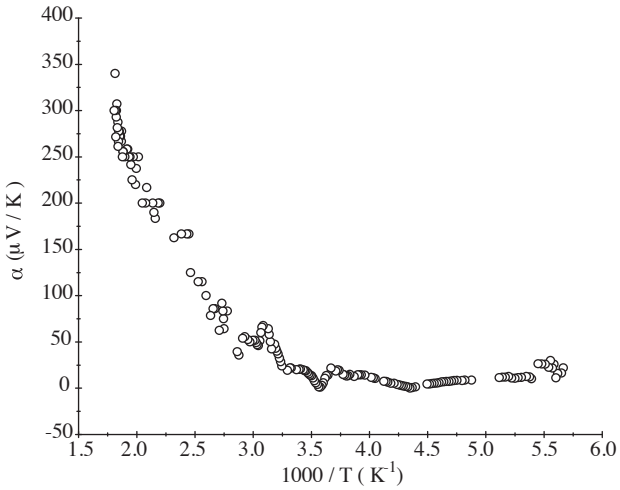

Figure 6. Relation between α and 10^3 /T for SnSe single crystal.

Another important parameter can be deduced with the aid of the obtained values of μ_n and μ_p using the Einstein relation, from which the diffusion coefficient for both carriers (holes and electrons) can be evaluated to be 195.89 and 570.06 $\mathrm{cm}^2/\mathrm{V}\cdot\mathrm{s}$, respectively.

From the intersection of the curve, the ratio between the effective masses of the electrons and holes can be estimated to be $\frac{m_n^*}{m_p^*} = 1.12 \times 10^{-3}$, assuming that this ratio does not vary with temperature.

In the impurity region the following equation can be applied [23]:

$$\alpha = \frac{k}{e}\left[A + Ln\frac{2(2\pi\, m_p^* kT)^{3/2} e\mu}{(2\pi h)^3}\right] - \frac{k}{e} Ln\, P. \tag{2}$$

Here, P is the hole concentration. The effective mass of the holes m_p^* is calculated from the relation between thermoelectric power and $\mathrm{Ln}\, P$. The relation is illustrated in Figure 7. As it is seen, α decreases linearly with increase in carrier concentration until reach the value 5.3 μV/K. Beyond this, the thermoelectric coefficient increases exponentially with increasing carrier concentration. Calculation of the effective mass of the holes from the intersection of the curve yields the value $m_p^* = 2.28 \times 10^{-29}$ kg. Combining these values with the above mentioned results for the ratio m_n^*/m_p^*, one obtains an effective mass of the electrons $m_n^* = 2.55 \times 10^{-32}$ kg. The results indicate that the electron mobility is much higher than the hole mobility. This is acceptable since the hole effective mass is much greater than that of electrons. The calculated values of the effective masses for both minority and majority carriers can be used to determine the relaxation time of both current carriers. Its value for holes comes to be 1.12×10^{-13} s, whereas for electrons it is 3.63×10^{-16} s. From the diffusion length $L = \sqrt{D\,\tau}$ the values of L_p and L_n are calculated and are found to be 4.66×10^{-6} cm and 4.54×10^{-7} cm for holes and electrons, respectively. Figure 8 shows the dependence of α on the natural logarithm of electrical conductivity according to the relation

$$\alpha = \frac{k}{e}\left[A + Ln\frac{2(2\pi\, m_p^* kT)^{3/2} e\mu}{(2\pi\, h)^3}\right] - \frac{k}{e} Ln\sigma. \tag{3}$$

It seems that the magnitude α is constant as the electrical conductivity increases in the lower conductivity region, up to temperature 272.5 K. Thereafter, α increases gradually reaching a maximum value at temperature 553 K.

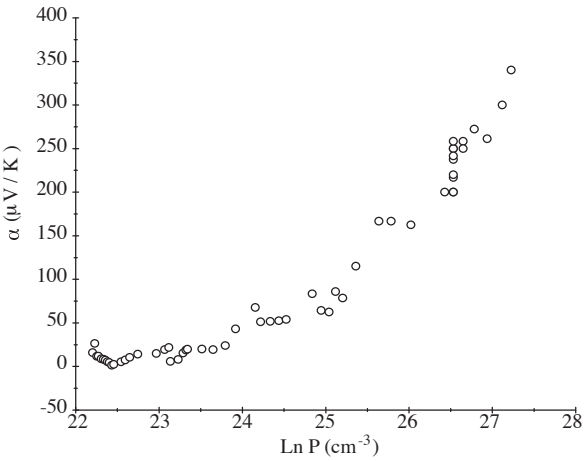

Figure 7. Relation between α and hole concentration of SnSe single crystal.

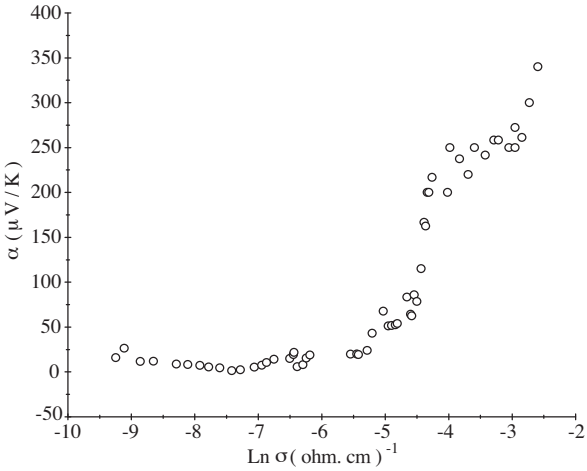

Figure 8. Variation of thermoelectric power with electrical conductivity for SnSe single crystal.

4. Conclusion

Electrical conductivity, hole coefficient and thermoelectric power properties of SnSe single crystal prepared by Bridgman technique have been studied.

The electrical measurements studied in the two crystallographic directions $\sigma_{||}$,s$\sigma_{\perp}$, parallel and perpendicular to the layers. The energy gap is determined in this study which values are 0.98 eV, 0.25 eV for both $\sigma_{||}$,sg$\sigma_{\perp}$, respectively.

The thermoelectric power measurements were performed with the direction of temperature gradient parallel to the layer plane.

From these measurements some of important parameters were determined such as the effective mass of electrons and hole, relaxation time and diffusion length of electrons and holes.

References

[1] T. Arai, M. Onomichi, Y. Mochida, and K. Kudo, *Akademiai Kiado. Budapest*, **51**, (1971).

[2] A. K. Garg, A. K. Jain, and O. P. Agnihotri, *Indian.J.Pure appl.phys.*, **21**, (1983), 276.

[3] J. G. Yu, A. S. Yue, and O. M. Stafsudd, *J.Crystal Growth*, **54**, (1981), 248.

[4] F. Lukes, E. Schmidt, J. Humlicek, P. Dub and F. Kosek, *Phys.stat.sol.(b)*, **137**, (1986), 569.

[5] H. R. Chandrasekhar, R. G. Humpreys, U. Zwicki, M. Cardona, *Phys.Rev.*, **B 15**, (1977), 2177.

[6] G. Valiukonis, F. M. Gashimzade, D. A. Guseinova, G. Krivaite, M. M. Mamedov and A. Sileika, *phys.stat.sol.(b)*, **122**, (1984), 623.

[7] R. Car, G. Ciucci, and L. Quartapelle, *phys.stat.sol.(b)*, **86**, (1978), 471.

[8] G. Ciucc, A. Guarnieri, G. L. Masserini and L. Quartapelle, *solid state commun.*, **29**, (1979), 75.

[9] F. M. Gashimzade, D. A. Guseinova, A. M. Kulibekov, I. K. Neimanzade and G. S. Orudzhev, Zonnaya struktura I spektr otrazheniya selenida germaniya, preprint No. **47**, Akad.Nauk Azerbaid.SsR, Inst.Fiz.Baku (1982) .

[10] H. R. Chandrasekhar, R. G. Humpreys, U. Zwicki, M. Cardona, *Phys.Rev.*, **15**, (1977), 2177.

[11] M. Taniguchi, R. L. Johnson, J. Ghijsen, M. Cardona, *Phys.Rev.*, **42**, (1990), 3634.

[12] J. M. Chamberlain, P. M. Nicolic, M. Merdan, P. Mihailovic, *J. Phys.C 9*, **L 637**, (1970).

[13] R. Eymard, A. Otto, *Phys.Rev.*, **16**, (1972), 1616 .

[14] G. Valiukonis, D. A. Guseinova, G. Krivaite, A. Sileika, *Phys.Stat.Sol.*, **135**, (1986), 299.

[15] Haluk Safak, Mustafa Merdan and O. Faruk Yuksel, *Turk J. Phys*, **26**, (2002), 341.

[16] Hiroaki Okamoto, P. R. Subramanian and Linda Kacprzak, *Binary Alloy Phase Diagrams.* ASM international (1996).

[17] G. A. Wiegers, W. Y. Zhou, *Mater.Res.Bull*, **26**, (1991), 879.

[18] S. A. Hussein, *Cryst.Res.Technol.*, **24**, (1989), 635.

[19] Weixin Zhang, Zeheng Yang, Juewen Liu, Lei Zhang, Zehua Hui, Weichao Yu, Yitai Qian, Lin Chen and Xianming Liu, *J. of Crystal Growth*, **217**, (2000), 157.

[20] R. N. Bhargava, *J.Crystal.Growth.*, **59**, (1982), 15.

[21] M. M. Nassary, M. K. Gerges, H. T. Shaban, A. S. Salwa, *Physica B*, **337**, (2003), 130.

[22] J. Lauc, *J. Phys. Rev.*, **95**, (1954), 1394.

[23] V. A. Chalbtov, *An Introduction to Semiconductors* (In Russian, 1969).